2009 American Control Conference
Hyatt Regency Riverfront, St. Louis, MO, USA
June 10-12, 2009

Reducing Vibration and Providing Robustness with Multi-Input Shapers

Joshua Vaughan and William Singhose

Abstract— **Input shaping is a command generation method that creates commands that result in low levels of residual vibration. This paper introduces new methods to design input shapers for multi-input systems. To justify the new methods, the multi-input vector diagram is used. Multi-input shaping design procedures are introduced that result in shapers that use secondary actuators to reduce vibration and increase robustness to modeling errors. Simulations of a nonlinear mobile tower crane model are used to illustrate the proposed method.**

I. Introduction

Input shaping reduces vibration by intelligently shaping the reference signals such that the vibratory modes are not excited [1], [2]. To implement this method, the reference signals are convolved with a sequence of impulses, called an input shaper. The timing and amplitudes of the impulses are determined using estimates of the system frequencies and damping. This process is demonstrated with a step command and a two-impulse Zero Vibration (ZV) input shaper in Fig. 1.

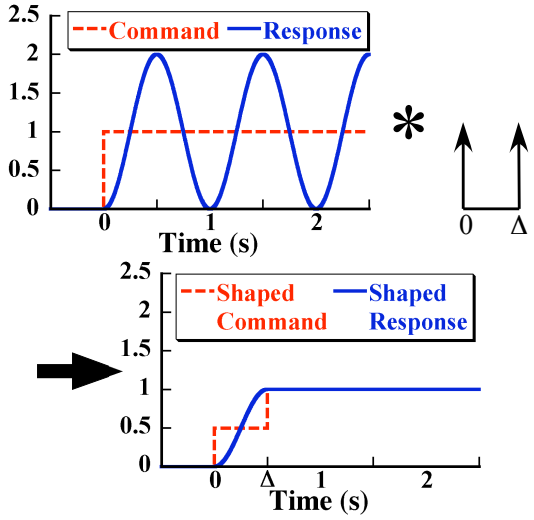

Fig 1. The Input Shaping Process

Although applying input shaping to multi-input systems can be straightforward, a few researchers have attempted to optimize the extension of input shaping to the multi-input domain. Some of the first published methods for optimized multi-input shaping relied on a zero-placement method to solve for multiple impulse sequences that are used with each input [3], [4]. Later works presented improvements on this initial algorithm [5], [6]. The original method, and the subsequent improvements, need somewhat accurate information about the influence of each input on the vibratory modes of the system.

The first improvement to this algorithm removed the impulse amplitude constraints from the original solution procedure, then scaled the resulting solution according to rigid body constraints [6]. This method generated marginally faster shapers than the original approach. An alternative improvement included additional robustness constraints, mentioned in the original work, but not implemented [5]. This work also proposed an adaptive multi-input shaping routine to account for situations when one or more inputs become zero. Limitations of this approach included possible actuator saturation and the ability to find a solution that meets both vibration and impulse amplitude requirements.

Other researchers have approached the problem by reformulating the problem as a quasi-convex optimization [7]–[9]. In each of these cases, the problem is transferred to the digital domain. Once in the digital domain, constraints on vibration and impulse amplitudes are created to form the optimization problem. Additional constraints can be added to the formulation to increase robustness and/or satisfy transient response requirements [9]. Only two previous papers have presented experimental results [9], [10].

The methods published thus far present several difficulties for practical implementation. The first is that the majority of the methods do not account for situations where one or more of the inputs is not used; the solutions require all actuators to be acting at all times. A second limitation is the requirement that each input shaper utilize an equal number of impulses, spaced equally in time. This limits the solution space. Finally, there is no explicit consideration of actuator limits in the methods published to date. In addition to these limitations, the solution procedures are typically much less intuitive than those for single input shapers.

This paper presents multi-input shaping methods that use multiple inputs to achieve performance that is not possible with a single input. Multi-input shapers are generated using a multi-input vector diagram, an extension of the vector diagram design technique used for single input systems [11]. These graphical design methods are discussed in Sections II and III. This paper will examine several classes of multi-input shapers. The first case uses secondary, compensating inputs to overcome the structural limitations of one primary input. Section IV outlines the design of such shapers using a multi-input vector diagram. The second class of multi-input shapers, introduced in Section V, use additional actuators to improve the robustness of the control system.

A mobile crane is used as the primary application example

All authors are with The George W. Woodruff School of Mechanical Engineering, Georgia Institute of Technology, Atlanta, GA, USA singhose@gatech.edu

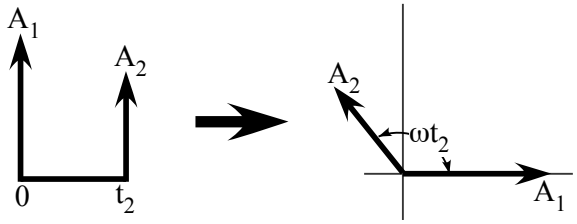

Fig 2. Representing Impulses on a Vector Diagram

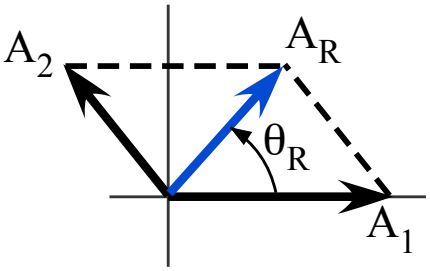

Fig 3. Resultant Vibration Vector from Adding Impulses

of multi-input shaping in this paper. However, the methods can be applied to other multi-input systems and are particularly well suited to overactuated systems, such as multi-stage positioning systems or hard disk drives. However, the methods presented in this paper assume a linear (or near linear) system. Extensions of the methods to systems that are highly nonlinear or non-stationary may require additional modifications.

II. Vector Diagrams

Due to the nonlinear nature of the constraints used to form input shapers, finding a solution to a complex formulation can be difficult. One tool that seeks to simplify the task is the vector diagram [11]. The vector diagram represents the vibration caused by an impulse as a vector. The vibration induced by an impulse sequence is represented by the sum of the sequence's representative vectors. The vector diagram can serve as both an input shaper analysis tool, as well as an input shaper design tool.

The process of representing an impulse sequence on a vector diagram is illustrated in Figure 2. Each impulse is plotted on the vector diagram in polar coordinates. The magnitude of each vector on the plot is simply the impulse magnitude. The angle of the i^{th} vector is:

$$\theta_i = \omega t_i \tag{1}$$

where ω is the vibration frequency, and t_i is the time of the i^{th} impulse. The time of the first impulse is always zero, so the resulting angle is zero as well. To plot a negative impulse, the vector simply points inward to the origin instead of outward. The angle is plotted in a manner just like positive impulses. Negative impulses are typically indicated with dashed lines.

To calculate the residual vibration caused by a sequence of impulses, the representative vectors are summed, as shown in Figure 3. The magnitude of the resultant vector, A_R, is proportional to the magnitude of the residual vibration caused by the impulse sequence. The angle of the resultant, θ_R, is equivalent to the phase shift of the residual vibration relative to vibration from a single impulse applied at time zero.

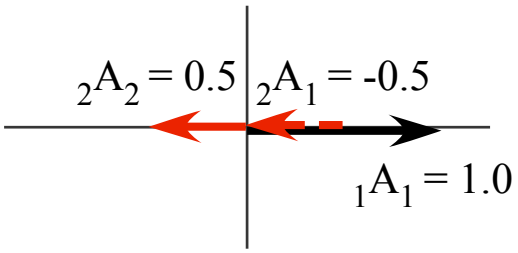

Fig 4. Multi-Input Vector Diagram

The vector diagram can also be used as an input shaper design tool. For example, a third vector can be added to the two shown in Figure 3 to produce zero vibration. This third vector is placed opposite of A_R. When it is placed this way, the three vectors will sum to zero, indicating the impulse sequence will excite zero vibration at the design frequency.

III. Multi-Input Vector Diagrams

This section presents an extension of the vector diagram to the multi-input domain. For clarity on multi-input vector diagrams, vectors must not only be designated according to their place in the impulse sequence, but also according to the input they are used to shape. Vectors are labeled ${}_kA_i$, where k represents the input they apply to and i represents their place in the impulse sequence for that input.

Figure 4 shows an example vector diagram for a multi-input shaper. The first input is applied to the system without any modification. This can be represented on the vector diagram as a unity magnitude vector at time zero, labeled ${}_1A_1$. To form an input shaper that results in zero vibration, vectors ${}_2A_1$ and ${}_2A_2$ are added to the diagram. Vector ${}_2A_1$ is located at time zero and has an amplitude of $-0.5({}_1A_1)$. Vector ${}_2A_2$ is located at time $\omega t_2 = \pi$ and has an amplitude of $0.5({}_1A_1)$. The sum of vectors ${}_1A_1$, ${}_2A_1$, and ${}_2A_2$ is a resultant vector of zero length, indicating that the sum of these two impulse sequences will result in zero vibration. The vectors in Fig. 4 were chosen to mimic the effect of a ZV shaper.

Any input shaper utilizing multiple actuators will be qualified with MI to indicate it is a multi-input shaped command. The shaped command created from the sum of inputs will be included after the MI designation. For example, if multiple actuators are combined to create a ZV shaped command, as in Fig. 4, it will be labeled MI-ZV.

Just as with a single-input vector diagram, there are an infinite number of choices to create impulse sequences that result in low levels of vibration. Fig. 5 shows another such choice. In this case, the vectors were all chosen to be unity magnitude (UM), and the sequence was chosen to match a UM-ZV shaper [12], [13].

Due to the large number of possible solutions conceived using vector diagrams, it makes an excellent tool to develop

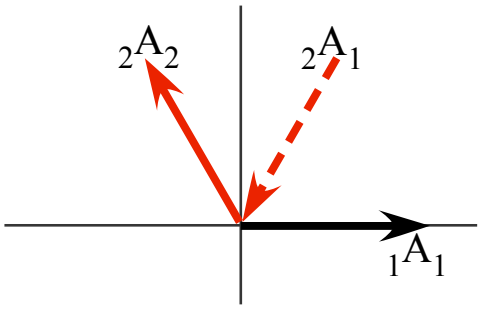

Fig 5. Multi-Input Vector Diagram – Unity Magnitude Impulse Constraints

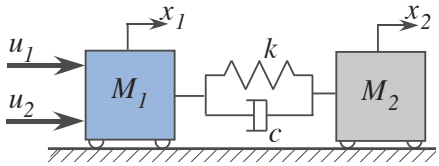

Fig 6. Simple Multi-Input Multi-Output Model

multi-input shapers. It provides a graphical representation of the ability to change impulse amplitudes and time locations to match physical system requirements.

It should be noted that multi-input vector diagram example above assumed that each impulse sequence was shaping a command that equally affected the vibratory mode. Proper scaling of the vector solutions and/or the inclusion of additional vectors allows the diagram to represent impulses applied to multiple inputs with unequal excitation effects. Also, the examples in this paper assume zero damping. Damping can be incorporated into multi-input vectors diagrams using the same methods as single-input vector diagrams [11].

IV. Design Using Multi-Input Vector Diagrams

This section presents design methods utilizing the multi-input vector diagram that can develop multi-input shapers for a wide variety of applications. The methods also provide the necessary tools to create shapers that are able to account for varying contributions between inputs and result in low vibration commands. A two-input, single-vibratory-mode system will be used first to demonstrate the use of the multi-input vector diagram. Examples from a full, nonlinear mobile tower crane model are then presented.

A. Compensating Inputs

One category of multi-input shapers is the class of shapers where the primary input driving the system cannot be properly shaped to eliminate vibration. However, a secondary input exists and can be properly shaped to cancel the vibration induced by the primary input. This method is particularly applicable to systems that are redundantly actuated, such as mobile cranes. For example, one primary actuator may be used to position the base of the system, while the secondary input(s) compensate for the vibration caused by the base motion.

To demonstrate the multi-input shaping principles, the two-mass-spring-damper model in Fig. 6 is utilized. The

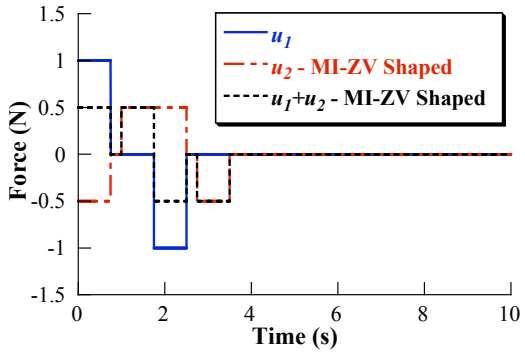

(a) Inputs

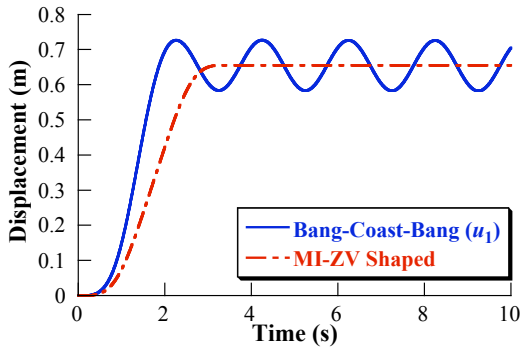

(b) Response of x_2

Fig 7. Responses to Unshaped and MI-ZV Commands

inputs are u_1 and u_2 and the outputs are the positions of M_1 and M_2, x_1 and x_2, respectively. The two masses are connected via a spring with spring constant k and damper with damping coefficient c. It is easy to see that the inputs affect the outputs identically.

A bang-coast-bang input from u_1, shown as a solid line in Fig. 7(a), will excite significant vibration in the system. This can been seen in the response of x_2, as shown by a solid line in Figure 7(b). Suppose that u_1 cannot be converted from an on-off function to a properly shaped function that produces low vibration. This could result from actuator limitations or limitations on the actuator force resolution. The multi-input vector diagram can be used to properly design the shaper for the second input, u_2, that compensates for the limitations of u_1. If each input is shaped according to the multi-input vector diagram shown in Fig. 4, then the sum of the two inputs, $u_1 + u_2$, is a properly shaped input. Note that u_1 is convolved with a single, unity magnitude impulse, which means it is unchanged. The bang-coast-bang function is then convolved with the impulses ${}_2A_1$ and ${}_2A_2$ to get the u_2 input. As seen in Fig. 7(a), the combination of $u_1 + u_2$ gives a properly shaped command. The response shown as a dashed line in Figure 7(b) demonstrates the effectiveness of this new Multi-Input ZV (MI-ZV) shaped command.

B. Scaling for Input Contributions

This section presents a method to scale the multi-input vector diagram solutions to create impulse sequences that account for the influence of each actuator. This procedure is

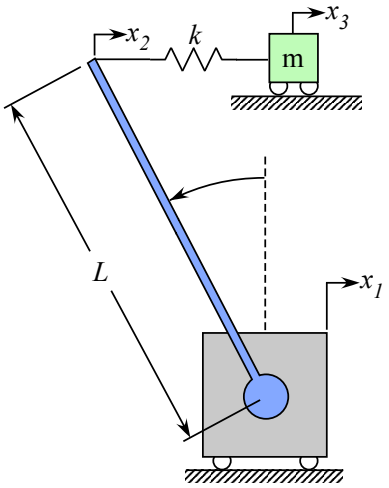

Fig 8. Simple Rotational Model

first demonstrated on an example system. Then, the general method is outlined.

The model in Fig. 8 represents a case where inputs have different effects on the output. It consists of a translational input, x_1, attached to a massless beam of length L. The second input to the system is the rotation of this beam, θ. A spring of stiffness k is attached to the end of the massless beam. The other side of the spring is attached to a mass, m, only capable of translational motion, x_3. This model is very similar to a mobile tower crane in which the centripetal effects of jib rotation are ignored.

The state-space form of the linearized equations of motion for the system is:

$$\dot{\bar{x}} = A\bar{x} + B\bar{u} \tag{2}$$

$$\dot{\bar{x}} = \begin{bmatrix} 0 & 1 \\ -\frac{k}{m} & 0 \end{bmatrix}\bar{x} + \begin{bmatrix} 0 & 0 \\ \frac{k}{m} & -\frac{k}{m}L \end{bmatrix}\begin{bmatrix} x_1 \\ \theta \end{bmatrix} \tag{3}$$

The model has two inputs, x_1 and θ, that do not equally affect the vibratory response of the system. The coefficients of the B matrix reveal how each input affects the system. As a result, they also provide insight into how multi-input shaper impulse sequences should be scaled.

The design of a multi-input shaper for this system begins with the multi-input vector diagram. One choice of impulses was shown in Fig. 4. For this system, the two sequences of impulses from this vector diagram are:

$$x_1 : \begin{bmatrix} A_i \\ t_i \end{bmatrix} = \begin{bmatrix} 1 \\ 0 \end{bmatrix} \tag{4}$$

$$\theta : \begin{bmatrix} A_i \\ t_i \end{bmatrix} = \begin{bmatrix} -0.5 & 0.5 \\ 0 & \frac{\pi}{\sqrt{\frac{k}{m}}} \end{bmatrix} \tag{5}$$

If these sequences are used directly on the system, without scaling, then the multi-input shaped commands actually excite more vibration than the unshaped, as seen in Fig. 9. This effect occurs because the vector diagram in Fig. 4 assumed that each input induces the same amplitude of vibration, but, in this case, they do not. To properly account for each input's influence on the output, the impulse amplitudes of

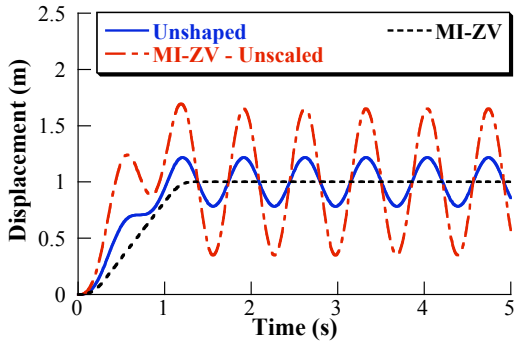

Fig 9. The Effects Multi-Input Shaping Impulse Scaling

each sequence are scaled according to the inverse of its corresponding entry in the B matrix. When this scaling is performed, the sequences become:

$$x_1 : \begin{bmatrix} A_i \\ t_i \end{bmatrix} = \begin{bmatrix} \frac{m}{k} \\ 0 \end{bmatrix} \tag{6}$$

$$\theta : \begin{bmatrix} A_i \\ t_i \end{bmatrix} = \begin{bmatrix} 0.5\frac{m}{kL} & -0.5\frac{m}{kL} \\ 0 & \frac{\pi}{\sqrt{\frac{k}{m}}} \end{bmatrix} \tag{7}$$

The sequences now properly account for the influence of each input on the vibratory dynamics of the system. However, the impulse amplitudes no longer sum to one. This means that the DC gain of the shaping process is not one. To correct the DC gain for this case, each impulse is multiplied by $\frac{k}{m}$, the inverse of the sum of the impulses from the two sequences. The scaled impulse sequences become:

$$x_1 : \begin{bmatrix} A_i \\ t_i \end{bmatrix} = \begin{bmatrix} 1 \\ 0 \end{bmatrix} \tag{8}$$

$$\theta : \begin{bmatrix} A_i \\ t_i \end{bmatrix} = \begin{bmatrix} 0.5\frac{1}{L} & -0.5\frac{1}{L} \\ 0 & \frac{\pi}{\sqrt{\frac{k}{m}}} \end{bmatrix} \tag{9}$$

The response of the system, using these two impulse sequences is shown by the dashed line in Fig. 9. The MI-ZV shaped response now exhibits no residual oscillation.

For systems with two inputs, this process is easily completed by scaling one of the impulse sequences by the ratio of coefficients from the B matrix. For this example, the θ impulse sequence could be scaled by:

$$\frac{B(2,1)}{B(2,2)} = \frac{\frac{k}{m}}{-\frac{kL}{m}} = -\frac{1}{L} \tag{10}$$

To generally apply the methods described above, the system must be represented in block diagonal form:

$$\dot{\bar{x}} = A\bar{x} + B\bar{u} \tag{11}$$
$$\bar{y} = C\bar{x}$$

where,

$$A = \text{blockdiag}[A_l] = \text{blockdiag}\begin{bmatrix} 0 & 1 \\ -\omega_l^2 & -2\zeta\omega_l \end{bmatrix} \tag{12}$$

$$B = \text{blockcol}\begin{bmatrix} 0 & 0 & \dots & 0 \\ b_1^l & b_2^l & \dots & b_k^l \end{bmatrix}, \quad l = 1, \dots, p$$

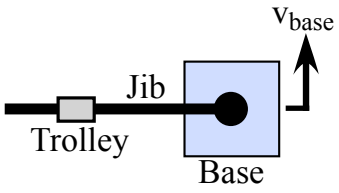

Fig 10. Multi-Input Shaping Example Configuration

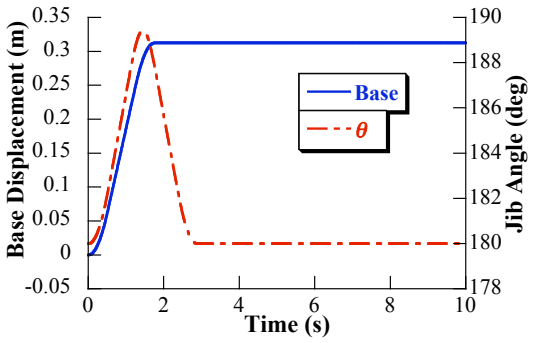

Fig 11. Multi-Input Shaping Commands for Full Tower Model

where there are k inputs to the system, p is the number of modes, and ω_l and ζ_l represent the frequency and damping ratio of the l^{th} mode, respectively. Placing the system in this form allows the influence of each input on each vibratory mode to be determined. To eliminate vibration for multiple modes of vibration, vector diagrams representing each mode must be examined simultaneously.

Using this method, multi-input commands were generated for a full, nonlinear mobile tower crane model, using a combination of base motion and jib rotation [14]. To establish a benchmark command and response, only base motion was used with the jib held perpendicular to the base velocity, as shown in Fig. 10. For the MI-ZV shaped case, the same base command was used, but the jib was rotated to eliminate the vibration caused by the base motion. For both cases, the suspension cable length, l, was set to 1.245m and the trolley position, r, at 0.8m. Both cable length and trolley position were held constant during the simulations. The natural frequency of oscillation is approximately 0.22Hz in this configuration. The base and slewing (θ) commands are shown in Fig. 11.

The unshaped and MI-ZV shaped payload responses are shown in Fig. 12. The unshaped base motion alone causes significant vibration in the β-direction, tangential to the jib, as seen in Fig. 12. Because the base motion is exactly perpendicular to the jib, no radial vibration is excited. The MI-ZV shaped case, utilizing jib slewing, is also shown in Fig. 12. The vibration in the β-direction, excited by the base motion, is eliminated. However, the centripetal effects of rotating the jib have excited a small level vibration in the radial direction. Despite this, the total amount of vibration is dramatically reduced.

The vector diagram is a powerful tool to visualize the vibration caused by an impulse sequence. However, it presents only one method to satisfy the vibration constraints. A more

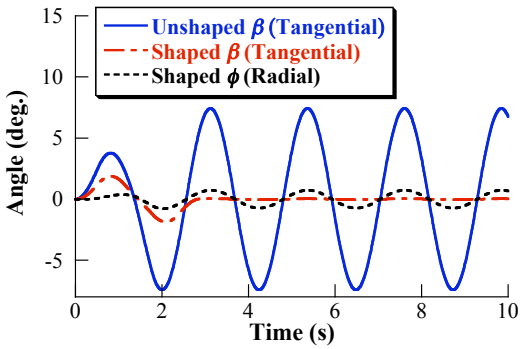

Fig 12. Full Tower Model Responses to Unshaped and MI-ZV Commands

general method may do so via an optimization routine. To summarize, the generalized algorithm for the procedure detailed in this section is:

1) Model the system in block diagonal form
2) Simultaneously solve for impulse sequences to satisfy vibration constraints for each vibratory mode
3) Scale resulting impulses according to the inverse of corresponding B-matrix entries
4) Check that the impulse sequences satisfy the rigid body constraints, and, if needed, apply uniform scaling to satisfy

In this generalized extension, the method becomes similar to those presented previously in the literature [3]–[9].

V. Adding Robustness via Secondary Actuation

In addition to combining inputs to create low-vibration commands when one input cannot be properly shaped, multi-input shapers can also be used to increase the robustness to modeling errors. The illustration of these methods will utilize the two-mass spring damper system shown in Fig. 6. Suppose that the first input, u_1, is only capable of the non-robust ZV shaped command. This scenario could result from a number of issues, namely a limited number of possible actuation states or other actuator limitations. In this case, the second input, u_2, can be designed such that the non-robust ZV command of u_1 is augmented by the secondary input, u_2, to create a more robust command. This process is shown in Fig. 13 for an initial ZV-shaped command that is converted to a robust Zero Vibration and Derivative (ZVD) [2] command, u_s, by the addition of a negative pulse in u_2.

The vibration at the design frequency will still reach a theoretical minimum of zero, as seen in Figure 14, but the command signal is more robust to errors in natural frequency. The benefit of the added robustness is shown in Figure 15, which shows the response of x_2 when there is a -20% modeling error in the frequency. The vibration resulting from the MI-ZVD command remains well below that of the ZV-shaped case, illustrating that it is more robust to errors in frequency.

VI. Conclusion

This paper presented methods to design multi-input shapers that utilize design techniques similar to those for

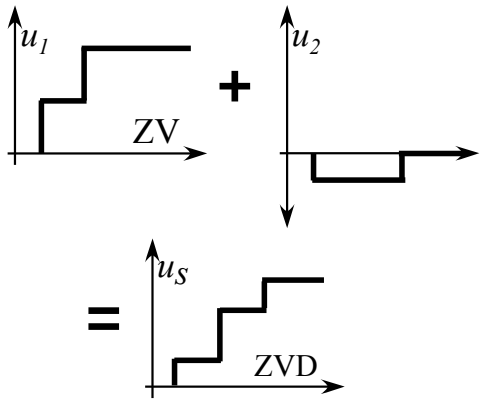

Fig 13. Compensation for Non-Robust Commands Utilizing Redundant Actuation

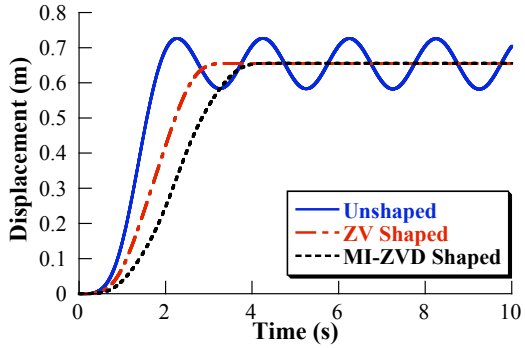

Fig 14. x_2 Responses to Unshaped, Base ZV-Shaped, and MI-ZVD commands

single input shapers. The multi-input vector diagram was introduced and used to design multi-input shapers. Methods of scaling these multi-input vector diagram solutions to account for the influence of each input on the vibratory dynamics were shown. In addition to creating multi-input shaped commands, a method was introduced that uses secondary actuators to increase the robustness of a single input-shaped command. Simulations of a nonlinear mobile tower crane illustrated key aspects of the proposed method.

ACKNOWLEDGEMENTS

The authors would like to thank Siemens Energy and Automation, Boeing Phantom Works, and the Hirose-Fukushima Laboratory at the Tokyo Institute of Technology for their support of this work.

REFERENCES

[1] O. Smith, *Feedback Control Systems*. New York: McGraw-Hill Book Co., Inc., 1958.

[2] N. C. Singer and W. P. Seering, "Preshaping command inputs to reduce system vibration," *Journal of Dynamic Systems, Measurement, and Control*, vol. 112, pp. 76–82, March 1990.

[3] L. Pao, "Input shaping design for flexible systems with multiple actuators," in *Proceedings of the 13th World Congress International Federation of Automatic Control*, San Francisco, CA, USA, 1997, pp. 267 – 72.

[4] L. Y. Pao, "Multi-input shaping design for vibration reduction," *Automatica*, vol. 35, pp. 81–9, 1999.

[5] M. D. Baumgart and L. Y. Pao, "Cooperative multi-input shaping for arbitrary inputs," in *Proceedings of 2001 American Control Conference*, vol. 1, June 2001, pp. 275–280.

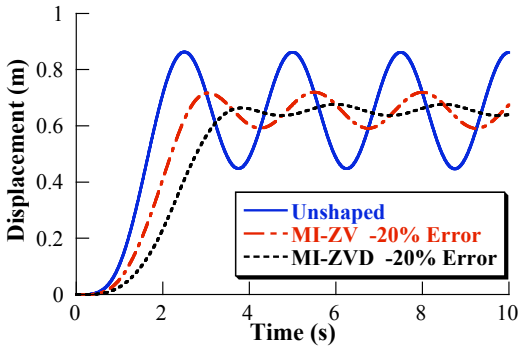

Fig 15. x_2 Responses to MI-Shaped Commands with -20% Frequency Error

[6] C. F. Cutforth and L. Y. Pao, "A modified method for multiple actuator input shaping," in *Proceedings of the 1999 American Control Conference*, vol. 1, 2-4 June 1999, pp. 66–70.

[7] M. D. Baumgart and L. Y. Pao, "Discrete time-optimal command shapers and controls for multi-input multi-output systems," in *Proceedings of 2002 American Control Conference*, vol. vol.3, May 2002, pp. 2279–84.

[8] ——, "Discrete time-optimal command shaping," *Automatica*, vol. 43, no. 8, pp. 1403 – 1409, 2007.

[9] S. Lim, H. Stevens, and J. How, "Input shaping design for multi-input flexible systems," *Journal of Dynamic Systems, Measurement and Control*, vol. 121, no. 3, pp. 443–7, 1999.

[10] J. Vaughan, W. Singhose, P. Debenest, E. Fukushima, and S. Hirose, "Initial experiements on the control of a mobile tower crane," in *ASME International Mechanical Engineering Congress and Exposition*, Seattle, Washington, 2007.

[11] W. Singhose, W. Seering, and N. Singer, "Residual vibration reduction using vector diagrams to generate shaped inputs," *ASME J. of Mechanical Design*, vol. 116, pp. 654–659, June 1994.

[12] W. Singhose, N. Singer, and W. Seering, "Time-optimal negative input shapers," *J. of Dynamic Systems, Measurement, and Control*, vol. 119, pp. 198–205, June 1997.

[13] S. S. Gurleyuk, "Optimal unity-magnitude input shaper duration analysis," *Archive of Applied Mechanics*, vol. 77, no. 1, pp. 63 – 71, 2007.

[14] J. Vaughan and W. Singhose, "Modeling and control of a mobile crane system," in *The Third International Conference for Advances in Mechanical Engineering and Mechanics*, Hammamet, Tunisia, 2006.